Numerical investigation of heat transfer of laminar and turbulent pulsating Al_2O_3/water nanofluid flow

S. Hoseinzadeh*
Centre for Asset Integrity Management, University of Pretoria, Pretoria, South Africa and Young Researchers and Elite Club, West Tehran Branch, Islamic Azad University, Tehran, Iran

P.S. Heyns
Centre for Asset Integrity Management, University of Pretoria, Pretoria, South Africa, and

H. Kariman
Faculty of Mechanical and Energy Engineering, Shahid Beheshti University, Tehran, Iran

*Corresponding author
S. Hoseinzadeh can be contacted at: hoseinzadeh.siamak@gmail.com

Abstract

Purpose – The purpose of this paper is to investigate the heat transfer of laminar and turbulent pulsating Al203/water nanofluid flow in a two-dimensional channel. In the laminar flow range, with increasing Reynolds number (Re), the velocity gradient is increased. Also, the Nusselt number (Nu) is increased, which causes increase in the overall heat transfer rate. Additionally, in the change of flow regime from laminar to turbulent, average thermal flux and pulsation range are increased. Also, the effect of different percentage of Al_2O_3/water nanofluid is investigated. The results show that the addition of nanofluids improve thermal performance in channel, but the using of nanofluid causes a pressure drop in the channel.

Design/methodology/approach – The pulsatile flow and heat transfer in a two-dimensional channel were investigated.

Findings – The numerical results show that the Al_2O_3/Water nanofluid has a significant effect on the thermal properties of the different flows (laminar and turbulent) and the average thermal flux and pulsation ranges are increased in the change of flow regime from laminar to turbulent. Also, the addition of nanofluid improves thermal performance in channels.

Originality/value – The originality of this work lies in proposing a numerical analysis of heat transfer of pulsating Al_2O_3/Water nanofluid flow -with different percentages- in the two-dimensional channel while the flow regime change from laminar to turbulent.

Keywords Nusselt number, Nanofluid, Reynolds number, Laminar and turbulent pulsating flow, Thermal performance, Al_2O_3/water nanofluid

Paper type Research paper

1. Introduction

Heat transfer is one of the essential processes in industry and consumer products. Increasing the efficiency of heat exchanger systems can significantly reduce the energy consumption of various methods and reduce greenhouse gas emissions (Hoseinzadeh *et al.*, 2019a; Hoseinzadeh and Azadi, 2017; Yousef Nezhad and Hoseinzadeh, 2017;

Javadi *et al.*, 2019; Hoseinzadeh, 2019). One thing that causes the reduction of heat transfer performance is the unfavorable thermophysical properties of fluids such as water and ethylene, which are used for heat transfer in the industry. These businesses inflict many limitations on cooling efficiency, and conventional methods to enhance cooling rates are insufficient (Hoseinzadeh *et al.*, 2018b; Chamkha, 2000; Takhar *et al.*, 1999; Sohani *et al.*, 2019; Sohani *et al.*, 2017; Sohani *et al.*, 2018; Sohani *et al.*, 2016; Moghimi *et al.*, 2010).

One of the ways to increase heat transfer is to use nanoparticles in the operating fluid (Dastan, 2017; Hoseinzadeh *et al.*, 2017a; Hoseinzadeh *et al.*, 2017b; Hoseinzadeh *et al.*, 2018a). Because their metal oxides such as Al_2O_3, CuO and TiO_2 have a higher conductivity (Hoseinzadeh *et al.*, 2017c; Mahdavi *et al.*, 2019; Dalvand and Moghadam, 2019; Goodarzi *et al.*, 2014; Goodarzi *et al.*, 2019b; Mehrabi *et al.*, 2012; Mehryan *et al.*, 2017; Selimefendigil *et al.*, 2018; Khodabandeh *et al.*, 2019; Zaib *et al.*, 2019; Dastan *et al.*, 2014), it can be expected that fluids containing solid particles have higher thermal conductivity. (Umavathi *et al.*, 2010; Menni *et al.*, 2019; Chamkha, 2002a; Nemati and Moghimi, 2014; Chamkha, 1994).

Increased heat transfer by moderate flow pulsation has therefore been considered because vibrational behavior anyway occurs in many practical applications. Pulsating flow is one of the basic types of flows used in the analysis of the study of the sustainability of the laminar and turbulent flows.

Valueva and Purdin (2015) developed a pulsating laminar flow in a rectangular channel. They analyzed the effect of the aspect ratio of the rectangular channel sides channel on the pulsating flow.

Sundstrom and Cervantes (2018) experimentally studied hot film by pulsating source in the unsteady turbulent pipe. The result showed that the Reynolds stresses dependent on the amplitude of pulsation.

Suresh *et al.* (2012) studied on a laminar convective heat transfer by using Al_2O_3–Cu/water hybrid nanofluid. In this experimental work, the results showed that at Reynolds number of 1,730, a maximum Nusselt number enhancement was 13.56 per cent. Also, they concluded that Nusselt number and friction factor are in good agreement with their experimental data.

Persoons *et al.* (2012) studied heat sinks with forced convection in microchannels for cooling electronic device purpose. Their experimental results for the overall heat transfer enhancement compared to the steady flow. They concluded that in higher amplitudes, a significant heat transfer enhancement is observed.

Venkatraman *et al.* (2009) presented the effect of an inert insulating net geometry on the heat transfer characteristics numerically. Thy used CFD software for fully developed flow with constant temperature boundary conditions. They calculated the Nusselt number. The enhancement factors of the Nusselt number decrease 50 per cent as the number of longitudinal ribs increased from 4 to 14.

Yuan *et al.* (2016) investigated the effects of wall thermal inertia on heat transfer of pulsating laminar flow theoretically. They used Green's function to solve the fully developed flow and heat transfer. They analyzed the effects of the pulsation amplitude, heat flux and Nusselt number. Their results showed that the wall thermal inertia suppresses the oscillation of wall heat flux increases and Nusselt number. Also, they showed that the pulsating laminar flow could reduce the average Nusselt number. And, the Nusselt number reduction of pipe flow is remarkable, which is mainly caused by differences in thermal performances of the channels.

Habib *et al.* (2004), Chamkha and Selimefendigil (2018) and Kumar *et al.* (2010) studied numerical and experimental of turbulent pulsating pipe flows under uniform heat flux condition. They used FLUENT software, the Reynolds number ranged from 8,462 to 48,540 and the pulsating ranged from 1 to 29.5 Hz. Their results showed that the Nusselt number is affected by both pulsation frequency and Reynolds number. They showed that at medium pulsation frequency between 4.1 and 13.9 Hz with (Reynolds number 8,462-14,581), enhancements in mean Nusselt number were up to 50 per cent and a reduction was observed at Reynolds number more than 21,200. Also, they showed that a reduction in Nusselt number of up to 40 per cent was obtained at medium pulsation frequency between 4.1 and 13.9 Hz for (Reynolds number 21,208-48,543).

Chamkha and Selimefendigil (2018), Kumar *et al.* (2010), Kumar *et al.* (2010), Thumma *et al.* (2017) and Kumar *et al.* (2010) studied forced convective pulsating nanofluid flow numerically over a backward-facing step with different nanoparticle shapes. They observed that the average Nusselt number is a decreasing function of the Strouhal number. They used nanofluids with spherical particles in pulsating flow with steady flow configurations. The result showed that the Nusselt number enhancements were 30.24 and 27.95 per cent at the highest volume fraction.

There are several articles that compared the thermal performance of water, ethylene glycol, alumina and CuO, CNT nanofluids (Chamkha, 2002b; Hoseinzadeh *et al.*, 2019b; Hoseinzadeh *et al.*, 2019c; Goodarzi *et al.*, 2019a; Gholamalizadeh *et al.*, 2019; Safaei *et al.*, 2014; Mahdavi *et al.*, 2016; Sangashekan *et al.*, 2019; Chamkha *et al.*, 2015; Chamkha *et al.*, 2015; Chamkha, 2001; Umavathi *et al.*, 2005; Reddy and Chamkha, 2017) in microchannels and porous channels with different cross-sectional geometries (Armaghani *et al.*, 2019; Mansour *et al.*, 2014; Madhu *et al.*, 2016; Izadi *et al.*, 2018; Mahdy and Chamkha, 2015; Hajiyan *et al.*, 2019; Selimefendigil and Chamkha, 2019; Chamkha, 1997; Umavathi *et al.*, 2009; Armaghani *et al.*, 2014; Ghasemiasl *et al.*, 2018).

In this research, first of all, the effect of laminar/turbulent Reynolds number on heat flux and Nusselt number are studied. Then the pressure and velocity counters of pulsating Al_2O_3/water nanofluid and the temperature contours of different ranges of Al_2O_3/water nanofluids are investigated. At first, Reynolds of 200 has been considered and then Reynolds of 200-2,000 was investigated in the laminar flow range, and afterward, Reynolds of 3,000 was evaluated in the range of turbulent flow. The results are shown that the Al_2O_3/water nanofluid have a significant effect on the thermal properties of the different flow (laminar and turbulent).

2. Governing the equations and validation

The fundamental equations of the dynamics of fluids are based on the universal rules of conservation of mass, momentum and energy equations (Anderson, 2007):

$$\frac{\rho \partial}{\partial t} + \nabla.(\rho.V) = 0 \tag{1}$$

$$\rho \frac{DV}{Dt} = \rho F + \nabla . \Pi_{ij} \tag{2}$$

$$\frac{\partial E_t}{\partial t} + \nabla.E_t V = \frac{\partial Q}{\partial t} - \nabla.q + \rho f.V + \nabla.(\Pi_{ij}.V) \tag{3}$$

The third term on the right side of equation (3) represents the work done per volume unit by volume forces on the control volume. Assuming Newtonian fluid, this relationship is in the following compressed tensor form:

$$\Pi_{ij} = -p\,\delta_{ij} + \mu\left(\frac{\partial u_i}{\partial x_j} + \frac{\partial u_j}{\partial x_i}\right) + \delta_{ij}\acute{\mu}\frac{\partial u_k}{\partial x_k}, \tag{4}$$

where δ_{ij} is the Kronecker delta function (if $i = j$, then $\delta_{ij} = 1$ and if $i \neq j$, then$\delta_{ij} = 1$), u_i represents the velocity component in direction i. μ is the viscosity coefficient (dynamic viscosity) and $\acute{\mu}$ is the second coefficient of viscosity. To calculate the velocity, pressure, temperature, density, etc., in the flow field, the equations governing the field must be solved. In general, the governing equations for the continuous environment are Navier–Stokes equations (Anderson, 2007).

The relationships used to calculate the nanofluid properties are in accordance with the following relationships. The momentum equation (2) is expressed in terms of mean time quantities in the form of equation:

$$\rho\left(\frac{\partial \overline{u}_i}{\partial t} + \overline{u}_j\frac{\partial \overline{u}_i}{\partial x_j}\right) = \overline{B}_i - \frac{\partial \overline{P}}{\partial x_i} + \frac{\partial}{\partial x_j}\left(\mu\frac{\partial \overline{u_i}}{\partial x_j} - \rho\overline{u_i^{'}u_j^{'}}\right) \tag{5}$$

The only difference between the equation obtained and momentum equation with instantaneous quantities is the addition of the last term to the right side of the equation above, i.e. $\rho\overline{u_i^{'}u_j^{'}}$. This term is called the turbulence stress or Reynolds stress (Hinze, 1975).

To model the fluid flow, it is necessary to solve the obtained equations completely and, on the other hand, the flow around the floaters is turbulent. In most flows with high Reynolds numbers, the effect of viscous forces is limited to the boundary layer. Gradually, owing to conditions caused by the geometric shape and flow field, such as surface roughness and pressure gradient, the pulsation of the fluid increases to the macroscopic surface and the flow becomes turbulent. With the advent of turbulence in the flow field, various physical phenomena are affected by the flow turbulence, most notably: momentum transfer, heat transfer and chemical reactions. Vortices in turbulent flows are always three-dimensional. Turbulence is a significant example of a highly nonlinear system which is associated with irregular and random properties. In this study, the input function of pulsating flow is:

$$u = u_{avg}(1 + A \cdot \sin(2\pi St\,\mathrm{t})) \tag{6}$$

The pulse flow function is as follows: an average of 0.0005 m/s, A is the pulsation amplitude equal to 1 and St denotes the Strouhal number with the value of 1.

2.1 Boundary conditions

According to the conditions of the problem, the inlet boundary of the solution zone consists of two separate parts of the input of the water and air, which must be separately defined. For this reason, from the very beginning, the input plate is divided into two parts by the waterline plate; the upper part of the waterline plate is the air inlet and the lower part is the water inlet. For the boundary condition of these two parts, we use the constant velocity condition. This constant velocity is also considered equal to the velocity of the floating model. Output flow conditions are also used for the output flow area. However, the constant velocity condition can also be used in the output but the length of the computational area behind the floater is large enough, so that this boundary condition can be used with high accuracy at the outlet. The symmetry boundary condition is used for the floating middle plane, which is the symmetry plate. Because the side and upper and lower boundaries are sufficiently far from the floating body, the flow effects at these points on the floating body are negligible, and thus a remote boundary condition can be used. Although the remote pressure can be used to create a distant boundary condition, but the wall condition is also acceptable and all of these boundaries can be assumed to be walls. The boundary condition of non-slip wall can be used for the floating wall.

2.2 Validation of the problem

The Nusselt number of the laminar pipe of circular channel with constant temperature is used for validation. Channel diameter is 0.1 m and channel length is 2 m. The Reynolds number is 200. Considering the Nusselt number, a circular pipe at the constant temperature state of 3.66 is used for solution validation and independence of network.

Because the computational fluid dynamic (CFD) simulations are carried out with ANSYS FLUENT software, given the diameter, conductivity of the fluid and the convection heat transfer coefficient, the Nusselt number is obtained (Yari *et al.*, 2015; Yari *et al.*, 2014; Hosseinzadeh *et al.*, 2017). In Figure 1, the Nusselt number is shown on the surface in terms of mesh size. According to the figure, 87,568 meshes are sufficient and the results are independent of the number of meshes.

Figure 2 shows the local Nusselt number based on the bulk temperature. As shown in the figure, because of the high temperature difference between the fluid and the wall at the beginning of the channel, more thermal flux is transferred to the fluid, which increases

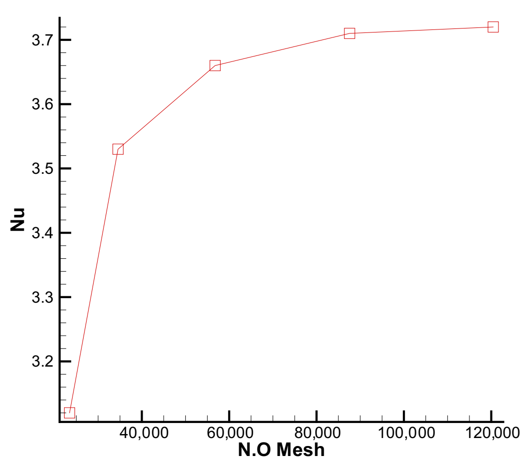

Figure 1. Nusselt number and mesh independency

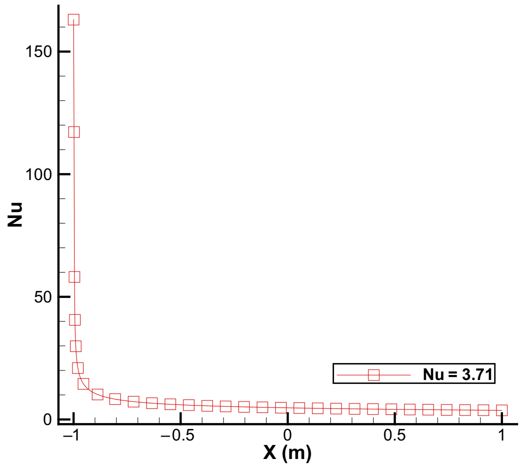

Figure 2. Local Nusselt number in circular channel

the Nusselt number. Approaching the output of channel, considering the increase in the fluid temperature and consequently the reduction of thermal flux, the Nusselt number decreases to a constant value.

3. Modeling of nanofluid

In this study, the Al_2O_3/water nanofluid is used as working fluid. There are similar relationships to calculate the density, specific heat capacity and thermal expansion coefficient as following equations:

$$\rho_{eff} = \rho_f(1-\varnothing) + \rho_s\varnothing \tag{7}$$

$$\left(\rho C_p\right)_{eff} = \left(\rho C_p\right)_f(1-\varnothing) + \left(\rho C_p\right)_f\varnothing \tag{8}$$

$$(\rho\beta)_{eff} = (\rho\beta)_f(1-\varnothing) + (\rho\beta)_f\varnothing \tag{9}$$

However, several models have been proposed for calculating nanofluids properties such as viscosity and thermal conductivity, as presented in the Appendix. In this study, the Maxwell's relation is used to calculate the thermal conductivity of nanofluid. Also, the Einstein's relation is used to calculate viscosity properties [equation (10)] (Einstein, 1911). The calculated properties for this nanofluid are presented in Table I:

Table I. Physical properties of Al_2O_3 nanofluid at different volume percentages

Volume percentages	Density	Viscosity	Thermal conductivity	Heat capacity
0	1,000	0.001	0.6	4182
3	1,087	0.001075	0.651	3815
5	1,145	0.001125	0.684	3601.4

$$\mu_{\mathrm{eff}} = (1 + 2.5\phi_{\mathrm{p}})\ \mu_{\mathrm{b}} \tag{10}$$

4. Results and discussion

4.1 Effects of laminar and turbulent flow

According to Figure 3, in the laminar flow range, the boundary layer decrease with increasing Reynolds number from 200 to 2000. Also, the velocity gradient and the Nusselt number are increased, which is the reason for an increase in the overall heat transfer rate and total Nusselt number.

As we know, the heat transfer coefficient in turbulent and also chaotic flows is higher than the heat transfer coefficient in laminar flow. So, every instrument that helps to cause the flow to turbulence or chaos will increase the heat transfer coefficient, whether the flow inside the pipe or on the pipe. Because of the formation of vortices and increased flow mixing in turbulent flow, especially in the boundary layer section, the heat transfer increases. There are several ways to create a vortex in the flow. By increasing the velocity component, which can endanger the flow stability, the flow becomes turbulence and the heat transfer increases. As can be seen in Figures 4 and 5, with the change of flow regime from laminar to turbulent, average thermal flux and pulsation ranges are increased.

Figures 6 (a), (b), (c), (d) and (e) show the velocity counters on the middle of the tube with different times as (6a; Time = 2.0000e−01), (6 b; Time = 4.0000e−01), (6c; Time = 6.0000e−01), (6d; Time = 8.0000e−01) and (6e; Time = 1.0000e + 00) that changes periodically. Also, the velocity inside the tube changes as the input velocity changes over the time. As can been seen, the maximum velocity at the inlet boundary is lower than the rest of the route. Plus, the maximum velocity is increased by expanding the boundary layer inside the tube.

Figures 7 (a), (b), (c), (d) and (e) shown the pressure contours of an input oscillation cycle for different times as (7a; Time = 2.0000e−01), (7 b; Time = 4.0000e−01), (7c; Time = 6.0000e−01), (7d; Time = 8.0000e−01) and (7e; Time = 1.0000e + 00). As expected as the pressure changes are very negligible. On the other hand, the pressure difference also fluctuates with velocity fluctuation, which is visible in the displayed counters.

Figures 8 (a), (b), (c), (d) and (e) shown the contours of surface Nusselt number in different times as (8a; Time = 2.0000e−01), (8 b; Time = 4.0000e−01), (8c; Time = 6.0000e−01), (8d; Time = 8.0000e-01) and (8e; Time = 1.0000e + 00). As we know, the dimensionless

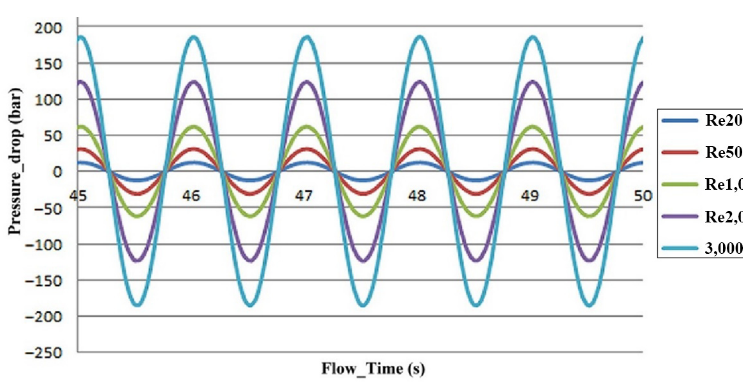

Figure 3. The effects of laminar and turbulent Reynolds number on the pressure drop

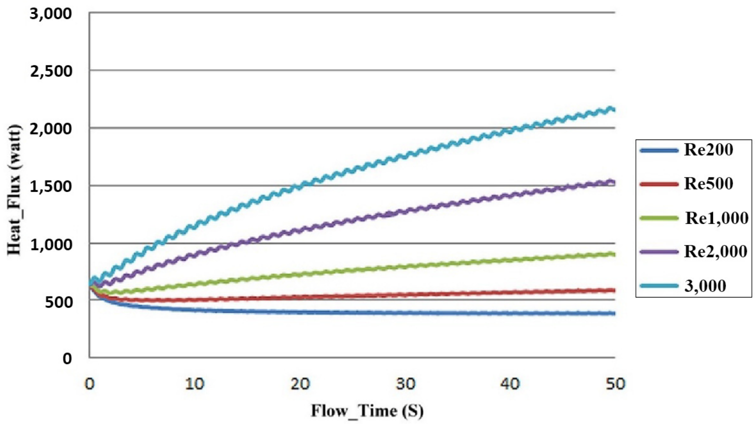

Figure 4. The effects of laminar and turbulent Reynolds number on the heat flux

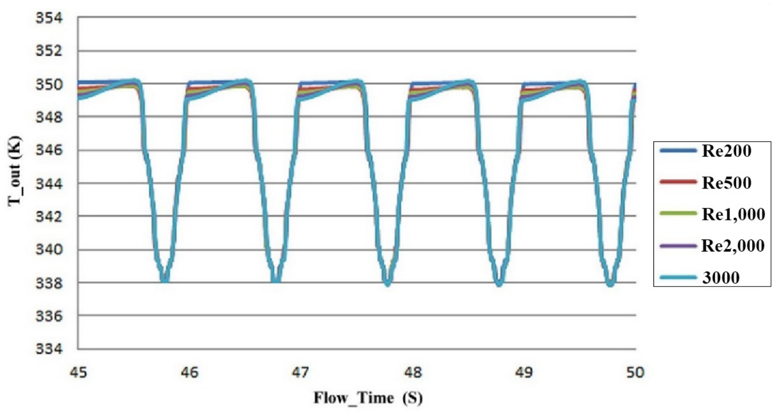

Figure 5. The effects of laminar and turbulent Reynolds number on the output temperature

Nusselt number represents the ratio of heat transferred through convection to heat transferred through conduction at the boundary of system.

As it can be seen in Figures 8 (a), (b), (c), (d) and (e), the heat transfer at the boundary is mostly via convection hear transfer at the beginning of the tube. On the other hand, the convection heat transfer share decreases relative to the conduction heat transfer $Nu_L = \frac{hL}{kf} = \frac{\text{Convective heat transfer coefficient}}{\text{Convective heat transfer coefficient}}$ as the boundary layer expands.

In the Figure 9 (a), (b) and (c), the changing temperature are compared with different volume percentages (0, 3 and 5 per cent) of Al_2O_3 nanofluid. As can be seen, the temperature on the surface increases during the pipe which causes a regular rise of temperature on the surface. Also, the fluid temperature is decreased by increasing the volume of Al_2O_3 nanoparticles inside the fluid while the energy input from the wall boundary is at a constant value. So, by increasing the percentage of Al_2O_3 nanofluid, it is possible to store more energy at a constant temperature.

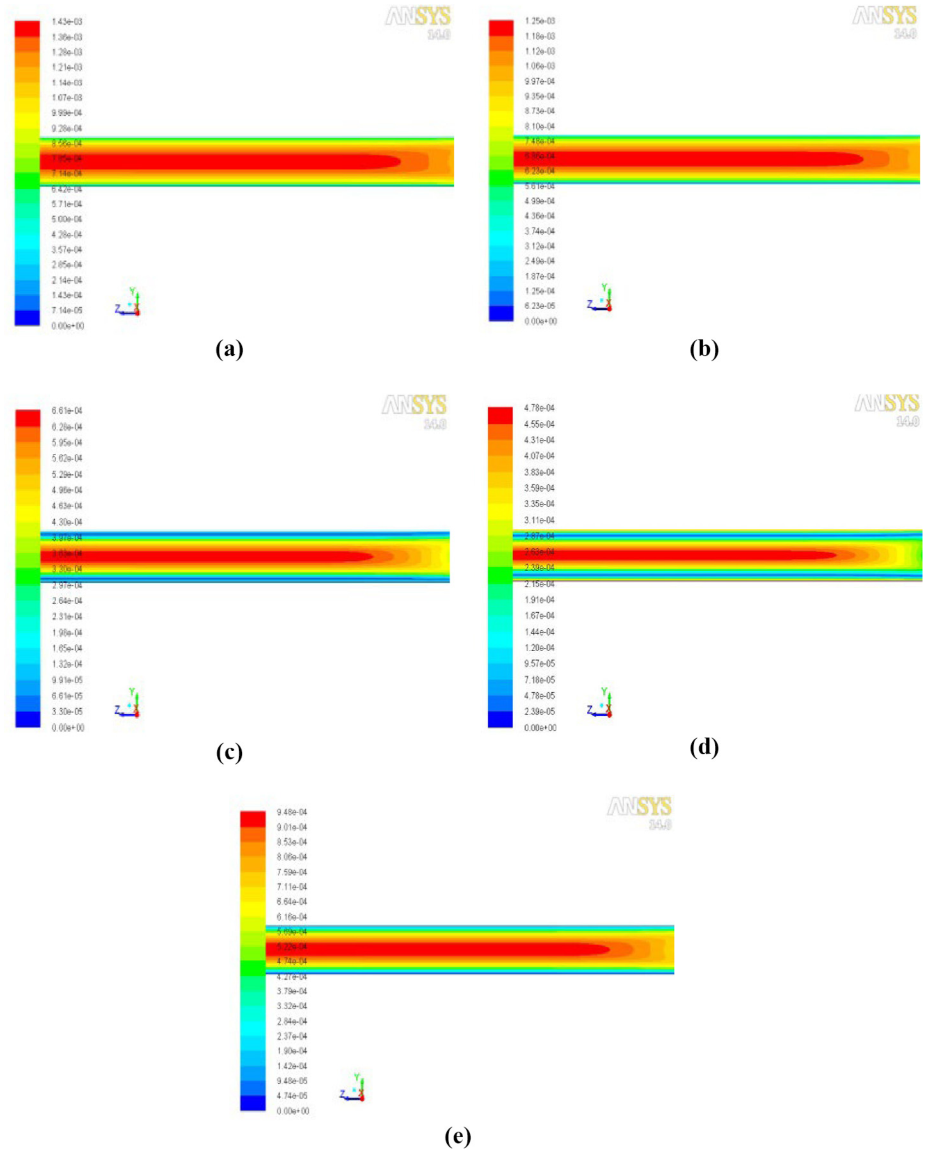

Figures 6. (a), (b), (c), (d) and (e) counters of velocity in different times

5. Conclusion

In this research, the effect of laminar (Reynolds number from 200 to 2,000) and turbulent (Reynolds number above 3,000) pulsating flow on heat transfer is investigated for two-dimensional channels. First of all, the effect of Al_2O_3/water nanofluid flow regime on output temperature, heat flux and Nusselt number are studied. After validation, the pressure and velocity counters of laminar and turbulent pulsating flow and influence of the Al_20_3

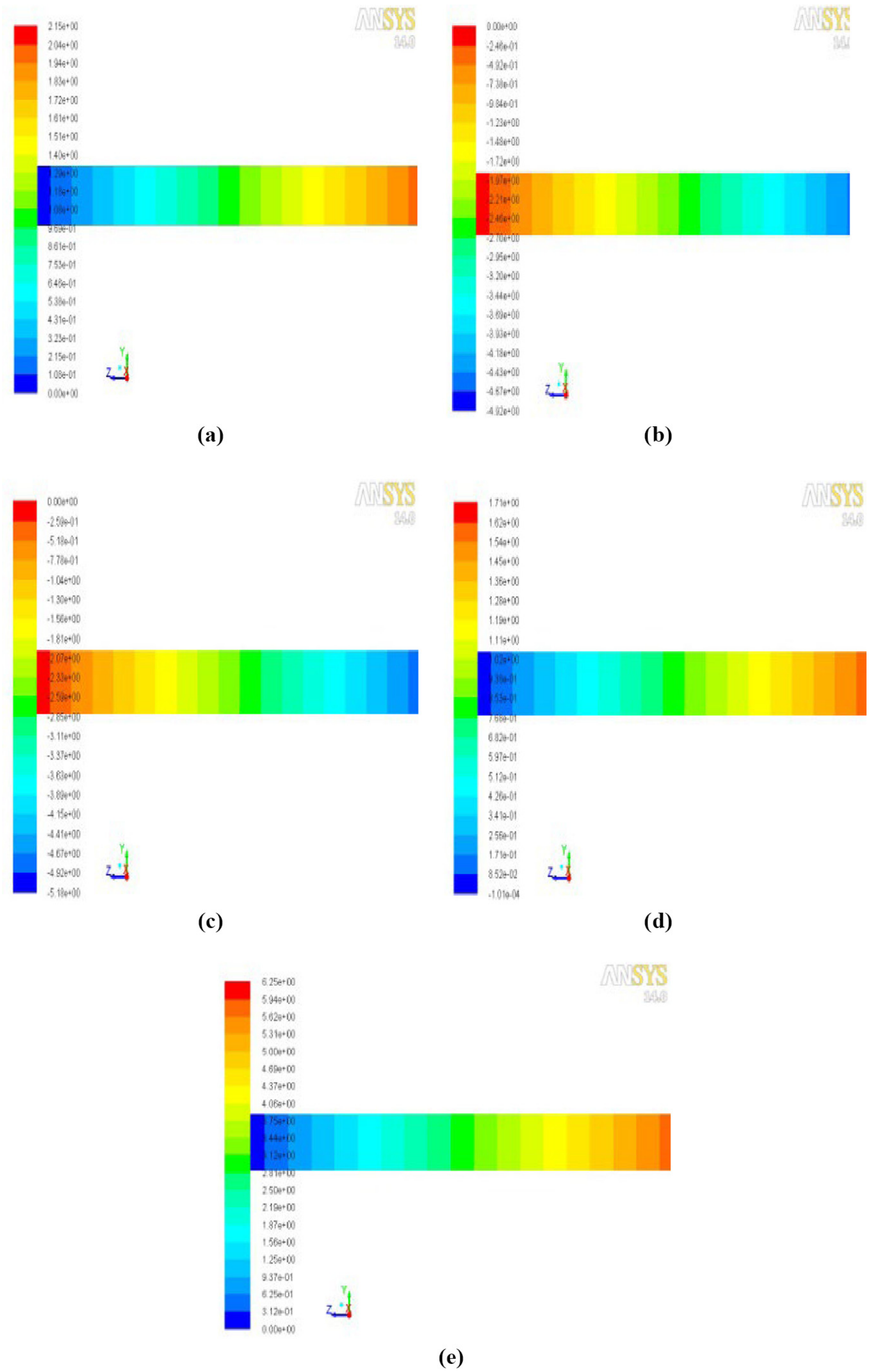

Figures 7. (a), (b), (c), (d) and (e) Counters of pressure in different times

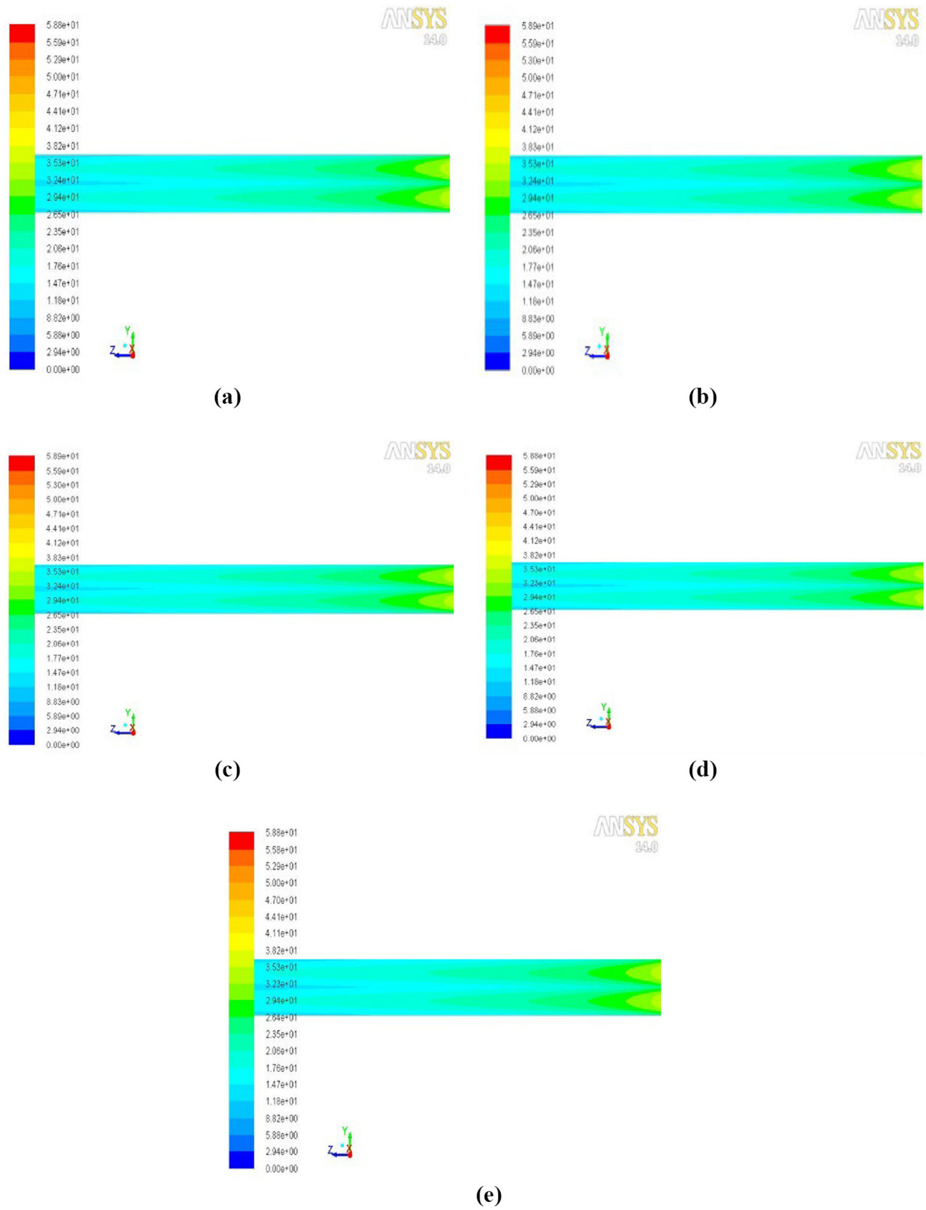

Figures 8. (a), (b), (c), (d) and (e) Contours of surface Nusselt number in different times

nanofluid at various volume percentages are investigated. The results show that the Al_2O_3/water nanofluid has a significant effect on the thermal properties in both flow (laminar and turbulent), and adding nanofluid improves thermal performance in channels, but using nanofluid causes a pressure drop in the channel.

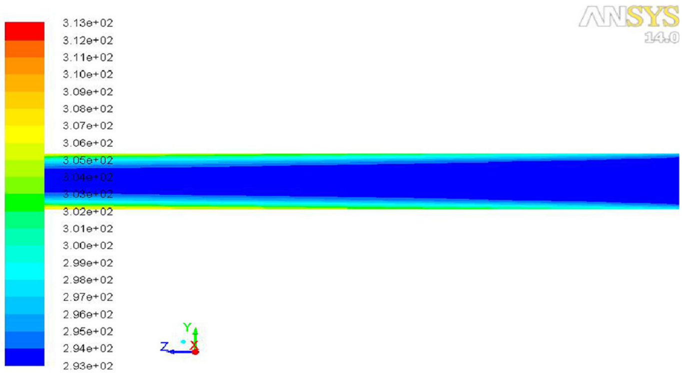

(a)

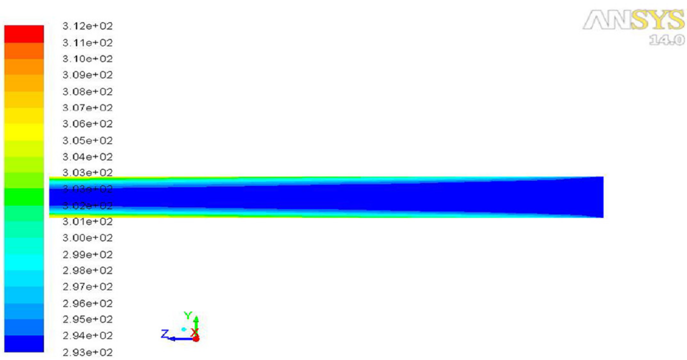

(b)

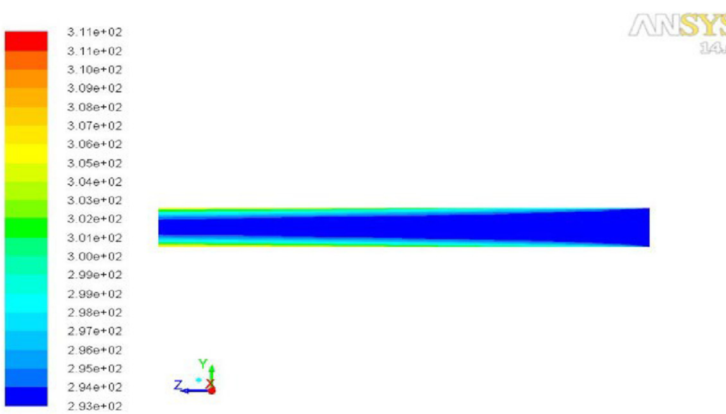

(c)

Notes: (a) 0%; (b) 3%; (c) 5%

Figure 9. (a), (b) and (c) temperature counters for different volume percentages of Al2O3 nanofluid

References

Anderson, J.D. (2007), *Fundamentals of Aerodynamics*, 4th ed., McGraw–Hill, London. ISBN 0-07-125408-0.

Armaghani, T., Chamkha, A.J., Maghrebi, M. and Nazari, M. (2014), "Numerical analysis of a nanofluid forced convection in a porous channel: a new heat flux model in LTNE condition", *Journal of Porous Media*, Vol. 17 No. 7, pp. 637-646.

Armaghani, T., Ismael, M.A., Chamkha, A.J. and Pop, I. (2019), "Mixed convection and entropy generation of an ag-water nanofluid in an inclined L-shaped channel", *Energies*, Vol. 12 No. 6, doi: 10.3390/en12061150.

Chamkha, J. (1994), "Unsteady flow of a dusty conducting fluid through a pipe", *Mechanics Research Communications*, Vol. 21 No. 3, pp. 281-288.

Chamkha, J. (1997), "Non-Darcy fully developed mixed convection in a porous medium channel with heat generation/absorption and hydromagnetic effects", *Numerical Heat Transfer; Part A: Applications*, Vol. 32 No. 6, pp. 653-675.

Chamkha, J. (2000), "The stokes problem for a dusty fluid in the presence of magnetic field, heat generation and wall suction effects", *International Journal of Numerical Methods for Heat and Fluid Flow*, Vol. 10 No. 1, pp. 116-133.

Chamkha, J. (2001), "Unsteady laminar hydromagnetic flow and heat transfer in porous channels with temperature-dependent properties", *International Journal of Numerical Methods for Heat and Fluid Flow*, Vol. 11 No. 5, pp. 430-448.

Chamkha, J. (2002a), "On laminar hydromagnetic mixed convection flow in a vertical channel with symmetric and asymmetric wall heating conditions", *International Journal of Heat and Mass Transfer*, Vol. 45 No. 12, pp. 2509-2525.

Chamkha, A.J. (2002b), "Flow of Two-Immiscible fluids in porous and nonporous channels", *Journal of Fluids Engineering*, Vol. 122 No. 1, p. 117.

Chamkha, A.J. and Selimefendigil, F. (2018), "Forced convection of pulsating nanofluid flow over a backward facing step with various particle shapes", *Energies*, Vol. 11 No. 11, available at: https://doi.org/10.3390/en11113068

Chamkha, A., Abbasbandy, S. and Rashad, A.M. (2015), "Non-Darcy natural convection flow for non-Newtonian nanofluid over cone saturated in porous medium with uniform heat and volume fraction fluxes", *International Journal of Numerical Methods for Heat and Fluid Flow*, Vol. 25 No. 2, pp. 422-437, available at: https://doi.org/10.1108/HFF-02-2014-0027

Dalvand, H.M. and Moghadam, A.J. (2019), "Experimental investigation of a water/nanofluid jacket performance in stack heat recovery", *Journal of Thermal Analysis and Calorimetry* , Vol. 135 No. 1, p. 657 available at: https://doi.org/10.1007/s10973-018-7220-0

Dastan, D. (2017), "Effect of preparation methods on the properties of titania nanoparticles: solvothermal versus sol-gel", *Applied Physics A*, Vol. 123 No. 1, pp. 613-699.

Dastan, D., Londhe, P.U. and Chaure, N.B. (2014), "Characterization of TiO_2 nanoparticles prepared using different surfactants by sol–gel method", *Journal of Materials Science: Materials in Electronics*, Vol. 25, pp. 3473-3479.

Einstein, A. (1911), "Eine neue bestimmung der moleküldimensionen", *Annalen Der Physik*, Vol. 34, pp. 591-592.

Ghasemiasl, R., Hoseinzadeh, S. and Javadi, M.A. (2018), "Numerical analysis of energy storage systems using two phase-change materials with nanoparticles", *Journal of Thermophysics and Heat Transfer*, Vol. 32 No. 2, pp. 440-448, available at: https://doi.org/10.2514/1.T5252

Gholamalizadeh, E., Pahlevanzadeh, F., Ghani, K., Karimipour, A., Nguyen, T. and Safaei, M. (2019), "Simulation of water/FMWCNT nanofluid forced convection in a microchannel filled with porous material under slip velocity and temperature jump boundary conditions", *International*

Journal of Numerical Methods for Heat and Fluid Flow, available at: https://doi.org/10.1108/HFF-01-2019-0030

Goodarzi, M., Tlili, I., Tian, Z. and Safaei, M. (2019a), "Efficiency assessment of using graphene nanoplatelets-silver/water nanofluids in microchannel heat sinks with different cross-sections for electronics cooling", *International Journal of Numerical Methods for Heat and Fluid Flow*, available at: https://doi.org/10.1108/HFF-12-2018-0730

Goodarzi, H., Akbari, O.A., Sarafraz, M.M., Karchegani, M.M., Safaei, M.R. and Sheikh Shabani, G.A. (2019b), "Numerical simulation of natural convection heat transfer of nanofluid with Cu, MWCNT, and Al_2O_3 nanoparticles in a cavity with different aspect ratios ", *Journal of Thermal Science and Engineering Applications*, Vol. 11 No. 6, p. 061020.

Goodarzi, M., Safaei, M.R., Vafai, K., Ahmadi, G., Dahari, M., Kazi, S.N. and Jomhari, N. (2014), "Investigation of nanofluid mixed convection in a shallow cavity using a two-phase mixture model", *International Journal of Thermal Sciences*, Vol. 75, pp. 204-220.

Habib, M.A., Attya, A.M., Said, S.A.M., Eid, A.I. and Aly, A.Z. (2004), "Heat transfer characteristics and Nusselt number correlation of turbulent pulsating pipe air flows", *Heat and Mass Transfer*, Vol. 40 Nos 3/4, pp. 307-318.

Hajiyan, M., Mahmud, S., Biglarbegian, M., Abdullah, H.A. and Chamkha, A. (2019), "Effect of magnetic field-dependent thermal conductivity on natural convection of magnetic nanofluid inside a square enclosure", *International Journal of Numerical Methods for Heat and Fluid Flow*, Vol. 29 No. 4, pp. 1466-1489, available at: https://doi.org/10.1108/HFF-07-2018-0374

Hinze, J.O. (1975), *Turbulence*, 2nd ed., McGraw-Hill. ISBN 0-07-029037-7.

Hoseinzadeh, S. (2019), "Evaluation of a smart window with (WO3 + Ag) nanocomposite assisted cooling system on energy saving", *Micro and Nanosystems*, Vol. 11, doi: 10.2174/1876402911666190218145433.

Hoseinzadeh, S. and Azadi, R. (2017), "Simulation and optimization of a solar-assisted heating and cooling system for a house in Northern of Iran", *Journal of Renewable and Sustainable Energy*, Vol. 9, doi: 10.1063/1.5000288.

Hoseinzadeh, S., Ghasemiasl, R., Bahari, A. and Ramezani, A.H. (2017a), "n-type WO3semiconductor as a cathode electrochromic material for ECD devices", *Journal of Materials Science: Materials in Electronics*, Vol. 28, pp. 14446-14452.

Hoseinzadeh, S., Ghasemiasl, R., Bahari, A. and Ramezani, A.H. (2017b), "The injection of Ag nanoparticles on surface of WO3thin film: enhanced electrochromic coloration efficiency and switching response", *Journal of Materials Science: Materials in Electronics*, Vol. 28, pp. 14855-14863.

Hoseinzadeh, S., Ghasemiasl, R., Bahari, A. and Ramezani, A.H. (2018a), "Effect of post-annealing on the electrochromic properties of layer-by-layer arrangement FTO-WO3-Ag-WO3-Ag", *Journal of Electronic Materials*, Vol. 47 No. 7, pp. 3552-3559.

Hoseinzadeh, S., Ghasemiasl, R., Havaei, D. and Chamkha, A.J. (2018b), "Numerical investigation of rectangular thermal energy storage units with multiple phase change materials", *Journal of Molecular Liquids*, Vol. 271, pp. 655-660.

Hoseinzadeh, S., Hadi Zakeri, M., Shirkhani, A. and Chamkha, A.J. (2019a), "Analysis of energy consumption improvements of a zero-energy building in a humid mountainous area", *Journal of Renewable and Sustainable Energy*, Vol. 11 No. 1, doi: 10.1063/1.5046512.

Hoseinzadeh, S., Heyns, P.S., Chamkha, A.J. and Shirkhani, A. (2019b), "Thermal analysis of porous fins enclosure with the comparison of analytical and numerical methods", *Journal of Thermal Analysis and Calorimetry*, doi: 10.1007/s10973-019-08203-x.

Hoseinzadeh, S., Moafi, A., Shirkhani, A. and Chamkha, A.J. (2019c), "Numerical validation heat transfer of rectangular cross-section porous fins", *Journal of Thermophysics and Heat Transfer*, pp. 1-7.

Hosseinzadeh, S., Ostadhossein, R., Mirshahvalad, H.R. and Seraj, J. (2017), "Using simpler algorithm for cavity flow problem", *An International Journal (MECHATROJ)*, Vol. 1.

Hoseinzadeh, S., Sahebi, S.A.R., Ghasemiasl, R. and Majidian, A.R. (2017c), "Experimental analysis to improving thermosyphon (TPCT) thermal efficiency using nanoparticles/based fluids (water)", *European Physical Journal Plus*, Vol. 132.

Izadi, M., Mohebbi, R., Chamkha, A. and Pop, I. (2018), "Effects of cavity and heat source aspect ratios on natural convection of a nanofluid in a C-shaped cavity using lattice Boltzmann method", *International Journal of Numerical Methods for Heat and Fluid Flow*, Vol. 28 No. 8, pp. 1930-1955, available at: https://doi.org/10.1108/HFF-03-2018-0110

Javadi, M.A., Hoseinzadeh, S., Ghasemiasl, R., Heyns, P.S. and Chamkha, A.J. (2019), "Sensitivity analysis of combined cycle parameters on exergy, economic, and environmental of a power plant", *Journal of Thermal Analysis and Calorimetry*, doi: 10.1007/s10973-019-08399-y.

Khodabandeh, E., Toghraie, D., Chamkha, A., Mashayekhi, R., Akbari, O. and Rozati, S.A. (2019), "Energy saving with using of elliptic pillows in turbulent flow of two-phase water-silver nanofluid in a spiral heat exchanger", *International Journal of Numerical Methods for Heat and Fluid Flow*, available at: https://doi.org/10.1108/HFF-10-2018-0594

Kumar, J.P., Umavathi, J.C., Chamkha, A.J. and Pop, I. (2010), "Fully-developed free-convective flow of micropolar and viscous fluids in a vertical channel", *Applied Mathematical Modelling*, Vol. 34 No. 5, pp. 1175-1186.

Madhu, M., Kishan, N. and Chamkha, A. (2016), "Boundary layer flow and heat transfer of a non-Newtonian nanofluid over a non-linearly stretching sheet", *International Journal of Numerical Methods for Heat and Fluid Flow*, Vol. 26 No. 7, pp. 2198-2217, available at: https://doi.org/10.1108/HFF-02-2015-0066

Mahdavi, M., Sharifpur, M., Ghodsinezhad, H. and Meyer, J.P. (2016), "Experimental and numerical study of the thermal and hydrodynamic characteristics of laminar natural convective flow inside a rectangular cavity with water, ethylene glycol-water and air", *Experimental Thermal and Fluid Science*, Vol. 78, pp. 50-64, available at: https://doi.org/10.1016/j.expthermflusci.2016.04.029

Mahdavi, M., Garbadeen, I., Sharifpur, M., Ahmadi, M.H. and Meyer, J.P. (2019), "Study of particle migration and deposition in mixed convective pipe flow of nanofluids at different inclination angles", *Journal of Thermal Analysis and Calorimetry*, Vol. 135 No. 2, pp. 1563-1575, available at: https://doi.org/10.1007/s10973-018-7720-y

Mahdy, A. and Chamkha, A. (2015), "Heat transfer and fluid flow of a non-Newtonian nanofluid over an unsteady contracting cylinder employing Buongiorno's model", *International Journal of Numerical Methods for Heat and Fluid Flow*, Vol. 25 No. 4, pp. 703-723, available at: https://doi.org/10.1108/HFF-04-2014-0093

Mansour, M.A., Bakeir, M.A. and Chamkha, A. (2014), "Natural convection inside a C-shaped nanofluid-filled enclosure with localized heat sources", *International Journal of Numerical Methods for Heat and Fluid Flow*, Vol. 24 No. 8, pp. 1954-1978, available at: https://doi.org/10.1108/HFF-06-2013-0198

Mehrabi, M., Sharifpur, M. and Meyer, J.P. (2012), "Application of the FCM-based neuro-fuzzy inference system and genetic algorithm-polynomial neural network approaches to modelling the thermal conductivity of alumina-water nanofluids", *International Communications in Heat and Mass Transfer*, Vol. 39 No. 7, pp. 971-977, available at: https://doi.org/10.1016/j.icheatmasstransfer.2012.05.017

Mehryan, S.A.M., Kashkooli, F.M., Ghalambaz, M. and Chamkha, A.J. (2017), "Free convection of hybrid Al2O3-Cu water nanofluid in a differentially heated porous cavity", *Advanced Powder Technology*, Vol. 28 No. 9, pp. 2295-2305.

Menni, Y., Chamkha, A., Zidani, C. and Benyoucef, B. (2019), "Baffle orientation and geometry effects on turbulent heat transfer of a constant property incompressible fluid flow inside a rectangular channel", *International Journal of Numerical Methods for Heat and Fluid Flow*, available at: https://doi.org/10.1108/HFF-12-2018-0718

Moghimi, M.A., Kimiaeifar, A., Rahimpour, M. and Bagheri, G.H. (2010), "An analytical solution for the Marangoni mixed convection boundary layer flow", *Proceedings of the Institution of Mechanical Engineers, Part C: Journal of Mechanical Engineering Science*, Vol. 224 No. 6, pp. 1193-1202, available at: https://doi.org/10.1243/09544062JMES1945

Nemati, H. and Moghimi, M. (2014), "Numerical study of flow over annular-finned tube heat exchangers by different turbulent models", *CFD Letters*, Vol. 6 No. 3, pp. 101-112.

Persoons, T., Saenen, T., Van Oevelen, T. and Baelmans, M. (2012), "Effect of flow pulsation on the heat transfer performance of a minichannel heat sink", *Journal of Heat Transfer*, Vol. 134 No. 9, p. 091702.

Reddy, P.S. and Chamkha, A. (2017), "Heat and mass transfer analysis in natural convection flow of nanofluid over a vertical cone with chemical reaction", *International Journal of Numerical Methods for Heat and Fluid Flow*, Vol. 27 No. 1, pp. 2-22, available at: https://doi.org/10.1108/HFF-10-2015-0412

Safaei, M.R., Togun, H., Vafai, K., Kazi, S.N. and Badarudin, A. (2014), "Investigation of heat transfer enhancement in a forward-facing contracting channel using FMWCNT nanofluids", *Numerical Heat Transfer; Part A: Applications*, Vol. 66 No. 12, pp. 1321-1340, available at: https://doi.org/10.1080/10407782.2014.916101

Sangashekan, M., Asan, S. and Gilani, H.G. (2019), "Investigation of eosin B removal from aqueous solution employing combined graphene oxide adsorption and zinc oxide coagulation processes", *Fibers and Polymers* , Vol. 20 No. 7, p. 1411, available at: https://doi.org/10.1007/s12221-019-8542-7

Selimefendigil, F. and Chamkha, A.J. (2019), "MHD mixed convection of nanofluid in a three-dimensional vented cavity with surface corrugation and inner rotating cylinder", *International Journal of Numerical Methods for Heat and Fluid Flow*, available at: https://doi.org/10.1108/HFF-10-2018-0566

Selimefendigil, F., Oztop, H.F. and Chamkha, A.J. (2018), "Natural convection in a CuO–water nanofluid filled cavity under the effect of an inclined magnetic field and phase change material (PCM) attached to its vertical wall", *Journal of Thermal Analysis and Calorimetry*.

Sohani, A., Sayyaadi, H. and Hoseinpoori, S. (2016), "Modeling and multi-objective optimization of an M-cycle cross-flow indirect evaporative cooler using the GMDH type neural network", *International Journal of Refrigeration*, Vol. 69, pp. 186-204.

Sohani, A., Sayyaadi, H. and Mohammadhosseini, N. (2018), "Comparative study of the conventional types of heat and mass exchangers to achieve the best design of dew point evaporative coolers at diverse climatic conditions", *Energy Conversion and Management*, Vol. 158, pp. 327-345.

Sohani, A., Sayyaadi, H. and Zeraatpisheh, M. (2019), "Optimization strategy by a general approach to enhance improving potential of dew-point evaporative coolers", *Energy Conversion and Management*, Vol. 188, pp. 177-213.

Sohani, A., Zabihigivi, M., Moradi, M.H., Sayyaadi, H. and Hasani Balyani, H. (2017), "A comprehensive performance investigation of cellulose evaporative cooling pad systems using predictive approaches", *Applied Thermal Engineering*, Vol. 110, pp. 1589-1608.

Sundstrom, L.R.J. and Cervantes, M.J. (2018), "On the similarity of pulsating and accelerating turbulent pipe flows", *Flow, Turbulence and Combustion*, Vol. 100 No. 2, pp. 417-436, available at: https://doi.org/10.1007/s10494-017-9855-5

Suresh, S., Venkitaraj, K.P., Selvakumar, P. and Chandrasekar, M. (2012), "Effect of Al2O3–Cu/water hybrid nanofluid in heat transfer", *Experimental Thermal and Fluid Science*, Vol. 38, pp. 54-60.

Takhar, H.S., Chamkha, A.J. and Nath, G. (1999), "Unsteady flow and heat transfer on a semi-infinite flat plate with an aligned magnetic field", *International Journal of Engineering Science*, Vol. 37 No. 13, pp. 1723-1736.

Thumma, T., Chamkha, A. and Sheri, S.R. (2017), "MHD natural convective flow of nanofluids past stationary and moving inclined porous plate considering temperature and concentration gradients with suction", *International Journal of Numerical Methods for Heat and Fluid Flow*, Vol. 27 No. 8, pp. 1765-1794, available at: https://doi.org/10.1108/HFF-03-2016-0090

Umavathi, J.C., Chamkha, A.J. and Sridhar, K.S.R. (2010), "Generalized plain Couette flow and heat transfer in a composite channel", *Transport in Porous Media*, Vol. 85 No. 1, pp. 157-169.

Umavathi, J.C., Chamkha, A.J., Mateen, A. and Al-Mudhaf, A. (2009), "Unsteady oscillatory flow and heat transfer in a horizontal composite porous medium channel", *Nonlinear Analysis: Modelling and Control*, Vol. 14, pp. 397-415.

Umavathi, J.C., Kumar, J.P., Chamkha, A.J. and Pop, I. (2005), "Mixed convection in a vertical porous channel", *Transport in Porous Media*, Vol. 61 No. 3, pp. 315-335.

Valueva, E.P. and Purdin, M.S. (2015), "The pulsating laminar flow in a rectangular channel", *Thermophysics and Aeromechanics*, Vol. 22 No. 6, p. 733, available at: https://doi.org/10.1134/S0869864315060098

Venkatraman, M., Shimpalee, S. and Van Zee, J.W. (2009), "Effect of net geometry on the Nusselt number distribution for channel flow", *Numerical Heat Transfer Applications*, Vol. 55 No. 4, pp. 309-336.

Yari, A., Hosseinzadeh, S. and Galogahi, M.R. (2014), "Two-dimensional numerical simulation of the combined heat transfer in channel flow", *International Journal of Recent Advances in Mechanical Engineering*, Vol. 3 No. 3, pp. 55-67.

Yari, A., Hosseinzadeh, S., Golneshan, A.A. and Ghasemiasl, R. (2015), "Numerical simulation for thermal design of a gas water heater with turbulent combined convection", *ASME/JSME/KSME 2015 Joint Fluids Engineering Conference*, AJKFluids 2015, Vol. 1.

Yousef Nezhad, M.E. and Hoseinzadeh, S. (2017), "Mathematical modelling and simulation of a solar water heater for an aviculture unit using MATLAB/SIMULINK", *Journal of Renewable and Sustainable Energy*, Vol. 9 No. 6, doi: 10.1063/1.5010828.

Yuan, H., Tan, S., Wen, J. and Zhuang, N. (2016), "Heat transfer of pulsating laminar flow in pipes with wall thermal inertia", *International Journal of Thermal Sciences*, Vol. 99, pp. 152-160.

Zaib, A., Haq, R.U., Chamkha, A.J. and Rashidi, M.M. (2019), "Impact of partial slip on mixed convective flow towards a Riga plate comprising micropolar TiO2-kerosene/water nanoparticles", *International Journal of Numerical Methods for Heat and Fluid Flow*, Vol. 29 No. 5, pp. 1647-1662, available at: https://doi.org/10.1108/HFF-06-2018-0258

Appendix

Table AI. Models proposed in prediction of thermal conductivity coefficient

Model	Expressions	Remarks
Maxwell (1873)	$\frac{K_{eff}}{K_L} = \frac{K_s + 2K_L + 2(K_s - K_L)\phi_s}{K_s + 2K_L - (K_s - K_L)\phi_s}$	Spherical particles ϕ_s – solids volume fraction
Hamilton and Crosser (1962)	$\frac{K_{eff}}{K_L} = \frac{K_s + (n-1)K_L - (n-1)\phi_s(K_L - K_s)}{K_s + (n-1)K_f + \phi_s(K_L - K_s)}$	n depends on particle shape and Ks/KL, $n = 3/\psi$ for Ks/KL > ~100, $n = 3$ for other cases, ψ – sphericity
Jeffrey (1973)	$\frac{K_{eff}}{K_L} = 1 + \frac{3\phi_s(K_s/K_L - 1)}{K_s/KL + 2} + 3\phi_s^2 \times \left(\frac{K_s/K_L - 1}{K_s/K_L + 2}\right)^2 \cdot \left[1 + \frac{1}{4}\left(\frac{K_s/K_L - 1}{K_s/K_L + 2}\right) + \frac{3}{16}\left(\frac{K_s/K_L - 1}{K_s/K_L + 2}\right)\left(\frac{K_s/K_L + 2}{2K_s/K_L + 3}\right) + \ldots\right]$	High-order terms represent pair interactions of randomly dispersed particles
Davis (1986)	$\frac{K_{eff}}{K_L} = 1 + \frac{3(K_s/K_L - 1)\cdot\left[\phi_s + f\cdot\phi_s^2 + O\left(\phi_s{}^3\right)\right]}{(K_s/K_L + 2) - (K_s/K_L - 1)\phi_s}$	High-order terms due to pair interactions of randomly dispersed spheres, f = 2.5 and 0.5 for K_s/K_L=10 and ∞, respectively
Bruggeman (1935)	$\frac{K_{eff}}{K_L} = \left[(3\phi_s - 1)\frac{K_s}{K_f} + (2 - 3\phi_s) + \sqrt{\Delta}\right]/4$ $\Delta = (3\phi s - 1)^2(K_s/K_L)^2 + \left(2 - 3\phi s\right)^2 + 2\left(2 + 9\phi_s - 9\phi_s{}^2\right)(K_s/K_L)$	Spherical particles, interactions between particles considered, applicable to high concentrations